

UC Santa Barbara

UC Santa Barbara Previously Published Works

Title

Design of Polymeric Zwitterionic Solid Electrolytes with Superionic Lithium Transport

Permalink

<https://escholarship.org/uc/item/2wp9z2nn>

Journal

ACS Central Science, 8(2)

ISSN

2374-7943

Authors

Jones, Seamus D
Nguyen, Howie
Richardson, Peter M
[et al.](#)

Publication Date

2022-02-23

DOI

10.1021/acscentsci.1c01260

Peer reviewed

Design of Polymeric Zwitterionic Solid Electrolytes with Superionic Lithium Transport

Seamus D. Jones, Howie Nguyen, Peter M. Richardson, Yan-Qiao Chen, Kira E. Wyckoff, Craig J. Hawker, Raphaële J. Clément, Glenn H. Fredrickson, and Rachel A. Segalman*



Cite This: *ACS Cent. Sci.* 2022, 8, 169–175



Read Online

ACCESS |



Metrics & More

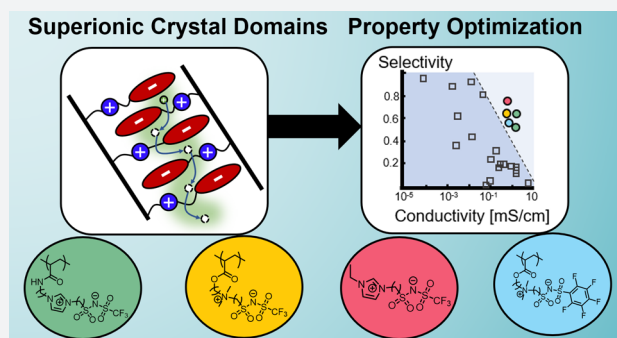


Article Recommendations



Supporting Information

ABSTRACT: Progress toward durable and energy-dense lithium-ion batteries has been hindered by instabilities at electrolyte–electrode interfaces, leading to poor cycling stability, and by safety concerns associated with energy-dense lithium metal anodes. Solid polymeric electrolytes (SPEs) can help mitigate these issues; however, the SPE conductivity is limited by sluggish polymer segmental dynamics. We overcome this limitation via zwitterionic SPEs that self-assemble into superionically conductive domains, permitting decoupling of ion motion and polymer segmental rearrangement. Although crystalline domains are conventionally detrimental to ion conduction in SPEs, we demonstrate that semicrystalline polymer electrolytes with labile ion–ion interactions and tailored ion sizes exhibit excellent lithium conductivity (1.6 mS/cm) and selectivity ($t_+ \approx 0.6$ –0.8). This new design paradigm for SPEs allows for simultaneous optimization of previously orthogonal properties, including conductivity, Li selectivity, mechanics, and processability.



have been identified that reliably surpass the conductivity of poly(ethylene oxide) (PEO), due to its combined low T_g and moderate salt solubility.^{7,11} Moreover, this solvation process often results in limited metal cation transport because strong cation–polymer interactions can slow down cation motion, especially for multivalent ions,¹² and thus cations frequently account for less than 20% of the total ionic current.¹³

INTRODUCTION

The efficient and safe storage of electrochemical energy is critical for such emerging technologies as electric vehicles and portable electronic devices.^{1–3} Practical requirements for next-generation secondary Li-ion batteries include higher energy densities and charge–discharge rates, which hinge on new high-voltage, high-capacity, and high-power cathode materials^{4–6} and on electrolytes with higher ionic conductivities (σ). Further, high energy densities can be reached only if Li-ion cells are operated over a wide potential range that exceeds the electrochemical stability window of current organic-solvent-based electrolytes. Next-generation Li-ion cells require the development of more stable and nonflammable electrolytes. Solid polymer electrolytes (SPEs) have attracted interest due to their stability and mechanical robustness,³ but it remains challenging to attain SPEs with both high ionic conductivity and lithium selectivity.⁷

Traditional SPEs, such as polyethers, exemplify vehicular ion transport (Figure 1a), where ion motion is controlled by the segmental relaxation time scale of the material (τ_g).^{8–10} This mechanism leads to the near-universal convergence of the measured ionic conductivities of rubbery amorphous polymers as a function of temperature when the latter is referenced to the glass transition temperature ($T - T_g$). Vehicular conduction limits polymer design because only plasticized (soft) polymer electrolytes display sufficiently high ion conduction for battery applications. In fact, no solid polymers

Inorganic solid-state electrolytes offer the strongest decoupling between mechanical and conductive properties. Although their atomic rearrangements are restricted by steep energy wells, they display ionic conductivities of 0.1–12 mS/cm and excellent cation selectivities ($t_+ \approx 1$).^{14–17} These attractive features result from ion diffusion channels comprised of interstitial and/or lattice site vacancies that can be designed to support ion hopping/migration. In addition, the rigidity and optimized size of these ion channels often completely prevent motion of nontarget ions (Figure 1B). Such materials are clearly advantageous for their high ionic conductivity, selectivity for target ions, and high elastic modulus, but they suffer from many challenges, such as poor contact at interfaces

Received: October 12, 2021

Published: January 4, 2022



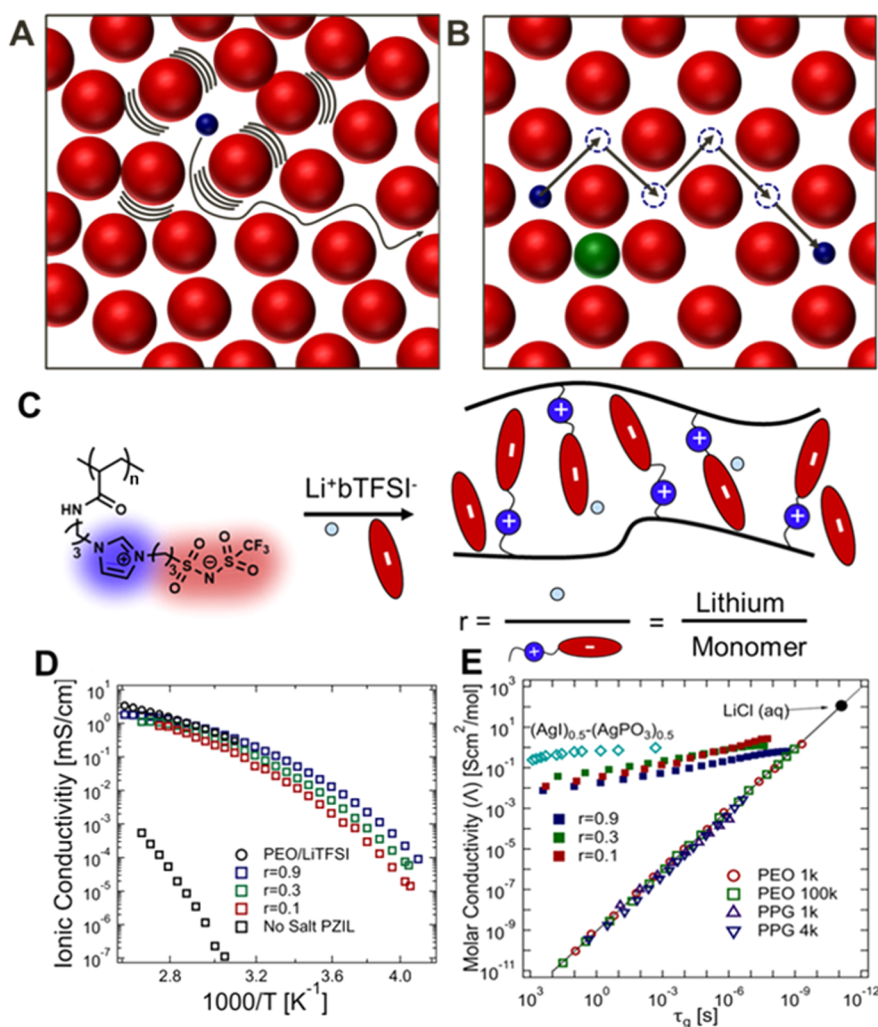


Figure 1. Schematic representation of the path of an ion through (A) a typical solid polymer electrolyte, in which ion transport is coupled to the time scale of local rearrangements, and (B) an ordered solid with sufficient free volume to enable superionic transport. The atoms of a crystal are typically confined to specific lattice positions, allowing sufficiently small ions with a low charge (blue spheres) to diffuse through the matrix (red spheres) via successive discrete hops involving vacant lattice sites or interstitial sites, while the motion of larger or highly charged ions (green sphere) is excluded. (C) The zwitterionic polymer studied herein comprises IL-inspired ions tethered to the backbone. Mobile ions are doped in through the addition of a Li⁺bTFSI⁻ salt at select molar ratios. (D) The DC ionic conductivity of salt-containing PZILs shown as a function of temperature is comparable to that of PEO (a best in class SPE).²⁸ (E) While standard SPEs have molar ionic conductivities coupled directly to the time scale of molecular rearrangements, ($\tau_g \sim 1/\Lambda$), the salt-containing ZILs demonstrate decoupling of these properties. Amorphous poly(ethylene oxide) (PEO) and poly(propylene glycol) (PPG) serve as reference SPEs, and (Ag)_{0.5}–(AgPO₃)_{0.5} as a typical superionic inorganic solid (literature data on PEO, PPG, and Ag systems obtained from Sokolov¹).

with the electrodes,¹⁸ brittleness and cracking,^{19,20} and limited chemical and electrochemical stability against a lithium metal anode and/or high-voltage cathode.²¹

The design of tough, processable polymers with ion conduction properties and elastic moduli comparable to those of inorganic electrolytes could mitigate the deficiencies of both SPEs and inorganic solid-state electrolytes. However, attempts to decouple conduction from segmental mobility in ion-conductive polymers have so far met with marginal success. Composites of inorganic particles and SPEs can partially mitigate issues encountered by each material class,^{22,23} but suffer from significant drawbacks, such as particle agglomeration and high impedance at the heterogeneous interfaces. Furthermore, the conductivity, selectivity, and mechanics of these composites typically result in only modest improvements over the constitutive SPE. Another approach to overcoming the rate limitations inherent to vehicular ion conduction in

traditional SPEs is to engineer disordered and dynamically heterogeneous polymers^{24,25} or microphase-separated block copolymer architectures with SPE channels that are integrated with a higher-modulus component.²⁶ Although these SPEs do exhibit decoupling from the vehicular conduction mechanism, their conductivity values have so far been well below those of state of the art SPEs. Recently it has been shown that crystalline ion channels in block copolymer electrolytes promote proton conduction, highlighting the possibility for ion transport through organic crystalline lattices.²⁷

To address these challenges, semicrystalline zwitterionic (ZI) SPEs are proposed. Key to their design is the decoupling of lithium transport from the fluidity of the matrix. This decoupling confers superionic performance resembling that of inorganic solid-state electrolytes, while the polymer matrix leads to processability and ductility akin to those of traditional polymeric electrolytes. We show here that facile lithium

transport is enabled by bulky cationic and anionic groups tethered to the backbone and arises from the weak interactions between lithium and framework ions. We further hypothesize that the disparity in size between lithium and constituent ions of the PZIL creates sufficient free volume for the superionic transport of Li^+ . The electrochemically determined ionic conductivity of this polymer electrolyte is competitive with that of state of the art polymeric ion conductors ($\sigma \approx 1.6$ mS/cm), despite its modest T_g value ($T_g \approx 270\text{--}300$ K). Significantly, ^7Li solid-state nuclear magnetic resonance (NMR) measurements indicate the presence of multiple lithium environments associated with different mobilities, suggesting an accelerated conductivity mode through crystalline domains. From the ^7Li and ^{19}F NMR self-diffusion coefficients obtained via pulsed field gradient NMR (PFG NMR), we calculate a lithium transport number of 0.67, which is markedly larger than the corresponding value for PEO ($t_+ \approx 0.2$).⁷ These results clearly illustrate the potential of polymeric zwitterionic liquids (PZILs) as new design platforms for solid polymer electrolytes with superionic conduction.

RESULTS AND DISCUSSION

PZILs Display a Faster-than-Vehicular Conduction Mechanism. To leverage the superionic conduction mechanisms characteristic of inorganic solid-state electrolytes, PZILs are designed with bulky, immobilized charges, resulting in labile ion–ion interactions and significant free volume for metal cation motion (Figure 1C). The choice of a bulky, pendant imidazolium-trifluoromethanesulfonamide (Im-TFSI) zwitterion allows for weaker Coulombic interactions, and the asymmetry in mobile cation and tethered anion sizes promotes crystal formation with sufficient void space for Li^+ ions. The orientation of the zwitterion (with the cation proximal to the backbone) is selected in accordance with calculations by Keith et al. which suggest that this orientation results in greater selectivity for lithium motion.²⁹ Although zwitterionic electrolytes have not been entirely unexplored,^{30–36} previous reports have leveraged amorphous polymers wherein ordering of the pendant zwitterions is not possible (often due to cross-linking of the network). These disordered systems do not display the superionic mechanism that distinguishes the PZILs reported herein. Recent studies have pointed toward the promising properties of zwitterions in electrochemical applications both as an ion transport matrix³⁷ and as a means to increase the dielectric constant of an electrolyte.³⁸

The choice of salt identity and concentration is critical to maximizing salt dissolution while preventing aggregation and precipitation. Mobile lithium bis(trifluoromethanesulfonimide) ($\text{Li}^+/\text{TFSI}^-$) is a highly labile salt whose use leads to facile dissociation in the presence of ion-solvating functionalities. It should also be noted that, due to the solvation afforded by zwitterionic liquid (ZIL) groups, salt/monomer molar ratios (parametrized by r) higher than the upper $r = 0.9$ value presented in Figure 1 can be obtained without salt precipitation (Section 6 in the Supporting Information).

Promising results were obtained from electrochemical impedance spectroscopy (EIS) measurements, with high ionic conductivities being observed for the PZILs and minimal conduction for the parent, undoped polymer (Figure 1D). This dramatic conductivity difference demonstrates that the ionic current is carried by the $\text{Li}^+/\text{TFSI}^-$ dopants, suggesting that the polymer acts as a fixed charged background for the mobile ions. The ionic conductivities of the PZILs are in excess of 1

mS/cm at elevated temperature, an important metric for practical implementation. Though other polymeric electrolytes, such as PEO, have exceeded this conduction threshold, their high values have been achieved via fast segmental motion.¹⁰ In contrast, the doped PZILs achieve competitive ion conductivities despite sluggish segmental motion, as indicated by their relatively high glass transition temperatures ($T_g \approx 270\text{--}300$ K; Section 7 in the Supporting Information). As a result, PZILs also maintain high ion mobilities at low temperatures below their T_g value. For example, the $r = 0.9$ sample has an ionic conductivity exceeding 10^{-2} mS/cm at 273 K ($1000/T = 3.6$), orders of magnitude larger than the conductivity of PEO at the same temperature ($<10^{-6}$ mS/cm)²⁸ (Figure 1D).

The ionic conduction behavior of the PZIL under small potentials and across a wide range of temperatures, including temperatures near and below T_g , differs from the standard, vehicular ion-conduction mechanism. The presence of superionic conduction is best indicated by the “Walden-plot” analysis shown in Figure 1E. Traditionally, the Walden rule predicts that the molar ionic conductivity ($\Lambda \equiv \sigma/c$, where c is the number density of charges in the electrolyte) is inversely proportional to the matrix viscosity.³⁹ In viscoelastic polymers, however, it is more appropriate to consider the glassy relaxation time of the polymer, τ_g , rather than the viscosity. Figure 1E demonstrates that the “polymeric Walden rule” (dashed black line), though an excellent predictor of conduction for PEO and poly(propylene glycol) (PPG, another polyether), dramatically underestimates the conduction of PZILs, particularly as the polymer approaches its T_g value ($\tau_g \rightarrow 100$ s). The Walden prediction ($\Lambda \sim D \sim \tau_g^{-1}$) is adapted from liquid-state electrolyte theory and corresponds to a conduction mechanism enabled by local fluid rearrangements. This prediction also distinguishes “superionic” from “subionic” conductors, where materials with conductivities exceeding the value expected from the Walden model are designated “superionic”. The conductivity behavior of the PZIL ($\tau_g(T)$, determined from rheology measurements; Section 1.7 in the Supporting Information) strongly deviates from Walden predictions, with ionic conductivities at the glass transition temperature ($\tau_g(T_g) = 100$ s) exceeding expectations by nearly 9 orders of magnitude. This decoupling is reminiscent of inorganic solids, such as superionic ceramics (we include $(\text{Ag})_{0.5}\text{-(AgPO}_3\text{)}_{0.5}$ as a reference in Figure 1E), which suggests that the PZILs exhibit a solid-like structural motif that enables superionic behavior.

The PZIL Ion Conduction Mechanism Arises from Ordered Subdomains That Promote Superionic Mobility. The superionic conductivity of the PZIL arises from ordered regions within the electrolyte, which act as pathways for facile, size-selective ion motion. Wide-angle X-ray scattering (WAXS) measurements demonstrate the presence of both ordered and amorphous features, as shown in Figure 2A and schematically represented in Figure 2B. The amorphous fingerprint manifests as a shouldered, broad peak in the q range $\sim 1\text{--}2.5$ \AA^{-1} . This amorphous halo reflects polymeric segment–segment correlations.^{40,41} The presence of sharper Bragg reflections that are most prominent in the absence of added salt and are weak at the highest salt loading suggests a structural order arising from the zwitterionic species, likely driven by electrostatic interactions between the zwitterions. This type of side-chain ordering has been reported in zwitterionic polymers^{42,43} and other systems.⁴⁴ The side-chain ordering in the present PZIL is confirmed by comparison

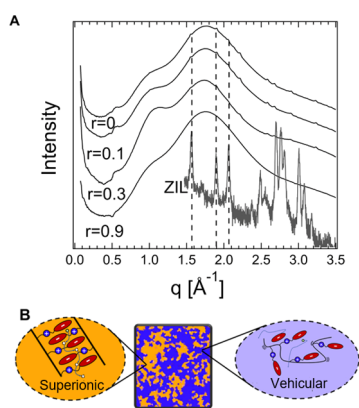


Figure 2. A structural analysis of the PZIL indicates the presence of two phases, one containing an ordered structure very similar to the small molecule on which the PZIL was based and another amorphous phase. (A) WAXS curves demonstrate the presence of amorphous and ordered structures within the PZIL sample. The crystalline peaks of a small-molecule analogue for this material appear to match well with the Bragg peaks of the PZIL, suggesting a structural similarity between the structure of the small-molecule crystal and the polymer. The small-molecule scattering conforms to the space group $Pna2_1$, as detailed in Section 4 in the Supporting Information. (B) Schematic representation of the conduction mechanism in the polymer suggested by NMR diffusometry. The amorphous domains are proposed to promote the motion of lithium and its counterion through vehicular motion; the ordered domains are suggested to have high selectivity for lithium, transported via a superionic conduction mechanism.

of the scattering pattern of the neat polymer ($r = 0$) with that of a small-molecule analogue of the pendant zwitterionic groups (Figure 2A). The structural similarity between the two crystalline structures is evident from the matching of the three primary peaks. The incomplete matching of higher-order peaks is unsurprising because the constraint of backbone attachment is likely to affect fine structural features. The similarity between the crystal structure of the small-molecule analogue and the polymer crystallites is further supported by a thermal analysis (Section 1.7 in the Supporting Information).

Our data show that these Im-TFSI based polymer electrolytes display two distinct diffusing environments, which may correspond to the “ordered” and “amorphous” regions of the PZIL. Further ^7Li and ^{19}F 1D NMR, NMR

relaxometry ($T_{1\rho}$), and pulsed-field gradient NMR (Section 9 in the Supporting Information) experiments allow atomic-scale insights into these transport environments and provide details on the supporting sub-micrometer diffusion processes. Significantly, in all three NMR measurements (Section 7 in the Supporting Information), we observe two distinct ^7Li populations with very different dynamics. These measurements consistently show that $\sim 25\%$ of the lithium exists in a “fast” environment that relaxes and diffuses nearly 1 order of magnitude more quickly than the second “slow” lithium population ($D_{\text{Li,fast}} = 7.6 \times 10^{-12} \text{ m}^2/\text{s}$, $D_{\text{Li,slow}} = 9.2 \times 10^{-13} \text{ m}^2/\text{s}$ at 358 K). Although these measurements cannot spatially distinguish motion through the amorphous and crystalline domains of the material, the presence of two lithium transport environments is suggestive of an inhomogeneous transport mechanism in which the ionic mobility of lithium is affected by the ordered domains of the electrolyte. In contrast, a ^{19}F NMR analysis reveals a single dynamic population of fluorine, suggesting that fluorine motion is not enhanced by the polymer’s dynamic heterogeneity. Due to the large size of the free TFSI⁻ anion, its motion may be hindered through the ordered regions of the electrolyte, as predicted by random barrier-type models of ion conduction (see Section 7 in the Supporting Information).

Conduction through Superionic Lattices Promotes High Cation Selectivity.

The performance of Li-ion batteries is ultimately dictated by the lithium-ion flux rather than by the total ionic conductivity of the electrolyte. A more complete picture of electrolyte performance, therefore, considers the selectivity of the electrolyte as well as its conductivity, with cation transport number and limiting current fraction (sometimes referred to as a transference number) being two practical metrics of electrolyte selectivity.^{45–47} The tradeoff between permeability (conductivity) and selectivity (limiting current fraction) can be captured via analogy to a Robeson plot typically used to characterize separation membranes, as shown in Figure 3.⁴⁸ A data aggregation study by Balsara and co-workers demonstrated a universal upper bound on the Robeson plot (reproduced in the dashed line of Figure 3A) that is independent of the polymer structure and backbone chemistry.⁷

As shown in Figure 3A, the PZILs reported here surpass the universal upper bound reported by Balsara and co-workers⁷ for polymer electrolytes, indicating an improvement in SPE design.

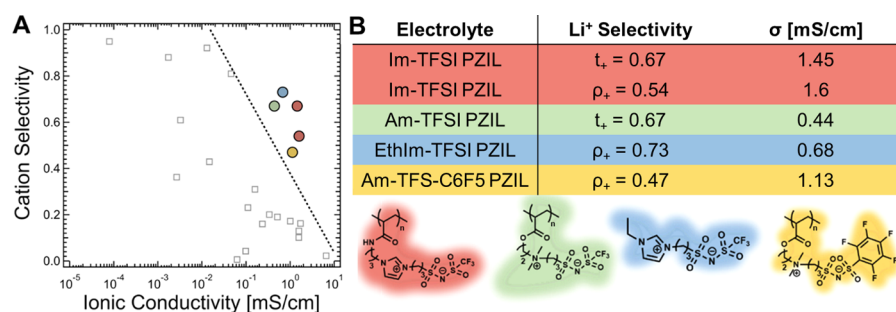


Figure 3. (A) A Robeson-inspired plot captures the traditional tradeoff between ionic selectivity (transference or transport number) versus permeability (conductivity). Unfilled symbols are values aggregated from a broad set of polymer electrolyte papers by Balsara and co-workers⁷ demonstrating the observed upper bound for these systems based on matrix molecular motion enabled ion transport. In comparison, the superionic PZILs studied here have comparable conductivities but much higher selectivities in comparison to the best conventional polymeric electrolytes. (B) The table indicates the selectivity metrics and conductivities for PZIL electrolytes. ρ_+ indicates the electrochemically determined limiting current fraction (Section 9 in the Supporting Information), and t_+ indicates the transport number determined by PFG-NMR (Section 7 in the Supporting Information). σ indicates the total ionic conductivity determined from EIS.

Both the cation transport number (t_+ , determined from PFG-NMR; see Section 7 in the Supporting Information) and the limiting current fraction (ρ_+ , evaluated for small potentials in Section 9 in the Supporting Information) indicate comparable lithium selectivities at 358 K of 0.67 and 0.54, respectively, for the PZIL discussed thus far (Im-TFSI PZIL). In an expansion of this design strategy, other PZILs (and a small-molecule ZIL, Figure 3B) with different cation/anion pairs demonstrate similar performance, and all exceed the previously observed upper bound in the Robeson-inspired plot. The simultaneously high conductivity and lithium selectivity of the PZIL suggests that engineering a solid-like and size-selective transport pathway into SPEs is a powerful strategy for outperforming the traditional “upper bound” of polymer electrolyte performance.

The grand challenge in the development of polymeric electrolytes has centered around designing electrolytes that are stiff, ionically conductive, and selective for lithium transport. Decades of work in polymer electrolyte research has suggested that ordered domains are deleterious for ion mobility within SPEs. This notion, however, is incompatible with superionic inorganic solid electrolytes, which depend on ordered lattices to enable selective ion motion. The present work demonstrates a new paradigm in which the advantageous mechanisms of inorganic electrolytes can be seamlessly integrated into organic polymers through the molecular engineering of ordered domains, resulting in SPEs with unprecedented lithium-ion conduction and selectivity. These systems provide powerful motivation for further studies of organic crystals and polymeric zwitterionic liquids as tunable platforms for the rapid and selective transport of target ions, though more studies are required to prove the in-operando stability of electrochemical cells based on these design principles.

■ ASSOCIATED CONTENT

SI Supporting Information

The Supporting Information is available free of charge at <https://pubs.acs.org/doi/10.1021/acscentsci.1c01260>.

Additional experimental details including materials and methods, NMR spectra and molecular characterization, electrochemical experimental results, and additional discussions (PDF)

■ AUTHOR INFORMATION

Corresponding Author

Rachel A. Segalman – Department of Chemical Engineering, Materials Research Laboratory, and Mitsubishi Chemical Center for Advanced Materials, University of California Santa Barbara, Santa Barbara, California 93110-5080, United States; Materials Department, University of California Santa Barbara, Santa Barbara, California 93110-5080, United States; orcid.org/0000-0002-4292-5103; Email: segalman@ucsb.edu

Authors

Seamus D. Jones – Department of Chemical Engineering, Materials Research Laboratory, and Mitsubishi Chemical Center for Advanced Materials, University of California Santa Barbara, Santa Barbara, California 93110-5080, United States

Howie Nguyen – Materials Department, University of California Santa Barbara, Santa Barbara, California 93110-5080, United States; orcid.org/0000-0002-3032-3674

Peter M. Richardson – Materials Research Laboratory and Mitsubishi Chemical Center for Advanced Materials, University of California Santa Barbara, Santa Barbara, California 93110-5080, United States

Yan-Qiao Chen – Materials Research Laboratory and Department of Chemistry and Biochemistry, University of California Santa Barbara, Santa Barbara, California 93110-5080, United States

Kira E. Wyckoff – Materials Research Laboratory, University of California Santa Barbara, Santa Barbara, California 93110-5080, United States; Materials Department, University of California Santa Barbara, Santa Barbara, California 93110-5080, United States

Craig J. Hawker – Materials Research Laboratory and Department of Chemistry and Biochemistry, University of California Santa Barbara, Santa Barbara, California 93110-5080, United States; Materials Department, University of California Santa Barbara, Santa Barbara, California 93110-5080, United States; orcid.org/0000-0001-9951-851X

Raphaële J. Clément – Materials Research Laboratory and Mitsubishi Chemical Center for Advanced Materials, University of California Santa Barbara, Santa Barbara, California 93110-5080, United States; Materials Department, University of California Santa Barbara, Santa Barbara, California 93110-5080, United States; orcid.org/0000-0002-3611-1162

Glenn H. Fredrickson – Department of Chemical Engineering, Materials Research Laboratory, and Mitsubishi Chemical Center for Advanced Materials, University of California Santa Barbara, Santa Barbara, California 93110-5080, United States; Materials Department, University of California Santa Barbara, Santa Barbara, California 93110-5080, United States; orcid.org/0000-0002-6716-9017

Complete contact information is available at: <https://pubs.acs.org/10.1021/acscentsci.1c01260>

Notes

The authors declare no competing financial interest.

■ ACKNOWLEDGMENTS

The research reported here was primarily supported by the National Science Foundation (NSF) through the Materials Research Science and Engineering Center at UC Santa Barbara, DMR-1720256 (IRG-2). For the synthesis and characterization of EthIm-TFSI and poly(Am-TFS-C6F5), we acknowledge financial support from the Mitsubishi Chemical Center for Advanced Materials (MC-CAM). We wish to acknowledge Professor Nitash Balsara, Professor Javier Read de Alaniz, and Dr. Oscar Nordness for helpful discussions related to this work. The NMR results reported here made use of the shared facilities of the UCSB MRSEC (NSF DMR 1720256), a member of the Materials Research Facilities Network (www.mfn.org). X-ray scattering measurements were performed at the National Synchrotron Light Source II (NSLS-II, beamline 11-BM, Brookhaven National Laboratory). XRD crystallography was performed at the UCSB X-ray Analytical Facility, S.D.J. wishes to thank Dr. Guang Wu for his guidance with single-crystal XRD.

REFERENCES

- (1) Bocharova, V.; Sokolov, A. P. Perspectives for Polymer Electrolytes: A View from Fundamentals of Ionic Conductivity. *Macromolecules* **2020**, *53* (11), 4141–4157.
- (2) Bruce, P. G.; Vincent, C. A. Polymer electrolytes. *Journal of the Chemical Society, Faraday Transactions* **1993**, *89* (17), 3187–3203.
- (3) Hallinan, D. T.; Balsara, N. P. Polymer Electrolytes. *Annu. Rev. Mater. Res.* **2013**, *43* (1), 503–525.
- (4) Ling, J.; Karuppiah, C.; Krishnan, S. G.; Reddy, M. V.; Misnon, I. I.; Ab Rahim, M. H.; Yang, C.-C.; Jose, R. Phosphate Polyanion Materials as High-Voltage Lithium-Ion Battery Cathode: A Review. *Energy Fuels* **2021**, *35* (13), 10428–10450.
- (5) Li, W.; Erickson, E. M.; Manthiram, A. High-nickel layered oxide cathodes for lithium-based automotive batteries. *Nature Energy* **2020**, *5* (1), 26–34.
- (6) Liang, G.; Peterson, V. K.; See, K. W.; Guo, Z.; Pang, W. K. Developing high-voltage spinel LiNi_{0.5}Mn_{1.5}O₄ cathodes for high-energy-density lithium-ion batteries: current achievements and future prospects. *Journal of Materials Chemistry A* **2020**, *8* (31), 15373–15398.
- (7) Galluzzo, M. D.; Maslyn, J. A.; Shah, D. B.; Balsara, N. P. Ohm's law for ion conduction in lithium and beyond-lithium battery electrolytes. *J. Chem. Phys.* **2019**, *151* (2), 020901.
- (8) Sun, J.; Stone, G. M.; Balsara, N. P.; Zuckermann, R. N. Structure–Conductivity Relationship for Peptoid-Based PEO–Mimetic Polymer Electrolytes. *Macromolecules* **2012**, *45* (12), 5151–5156.
- (9) Wang, Y.; Fan, F.; Agapov, A. L.; Yu, X.; Hong, K.; Mays, J.; Sokolov, A. P. Design of superionic polymers—New insights from Walden plot analysis. *Solid State Ionics* **2014**, *262*, 782–784.
- (10) Mongcopa, K. I. S.; Tyagi, M.; Mailoa, J. P.; Samsonidze, G.; Kozinsky, B.; Mullin, S. A.; Gribble, D. A.; Watanabe, H.; Balsara, N. P. Relationship between Segmental Dynamics Measured by Quasi-Elastic Neutron Scattering and Conductivity in Polymer Electrolytes. *ACS Macro Lett.* **2018**, *7* (4), 504–508.
- (11) Lee, B. F.; Kade, M. J.; Chute, J. A.; Gupta, N.; Campos, L. M.; Fredrickson, G. H.; Kramer, E. J.; Lynd, N. A.; Hawker, C. J. Poly(allyl glycidyl ether)-A versatile and functional polyether platform. *J. Polym. Sci., Part A: Polym. Chem.* **2011**, *49* (20), 4498–4504.
- (12) Park, B.; Schaefer, J. L. Review—Polymer Electrolytes for Magnesium Batteries: Forging Away from Analogs of Lithium Polymer Electrolytes and Towards the Rechargeable Magnesium Metal Polymer Battery. *J. Electrochem. Soc.* **2020**, *167* (7), 070545.
- (13) Hiller, M. M.; Joost, M.; Gores, H. J.; Passerini, S.; Wiemhöfer, H. D. The influence of interface polarization on the determination of lithium transference numbers of salt in polyethylene oxide electrolytes. *Electrochim. Acta* **2013**, *114*, 21–29.
- (14) Fu, J. Superionic conductivity of glass-ceramics in the system Li₂O–Al₂O₃–TiO₂–P₂O₅. *Solid State Ionics* **1997**, *96* (3), 195–200.
- (15) Bron, P.; Johansson, S.; Zick, K.; Schmedt auf der Günne, J.; Dehnen, S.; Roling, B. Li₁₀SnP₂S₁₂: An Affordable Lithium Superionic Conductor. *J. Am. Chem. Soc.* **2013**, *135* (42), 15694–15697.
- (16) Kamaya, N.; Homma, K.; Yamakawa, Y.; Hirayama, M.; Kanno, R.; Yonemura, M.; Kamiyama, T.; Kato, Y.; Hama, S.; Kawamoto, K.; Mitsui, A. A lithium superionic conductor. *Nat. Mater.* **2011**, *10* (9), 682–686.
- (17) Murugan, R.; Thangadurai, V.; Weppner, W. Fast lithium ion conduction in garnet-type Li₇La₃Zr₂O₁₂. *Angewandte Chemie (International ed. in English)* **2007**, *46* (41), 7778–81.
- (18) Zhang, W.; Richter, F. H.; Culver, S. P.; Leichtweiss, T.; Lozano, J. G.; Dietrich, C.; Bruce, P. G.; Zeier, W. G.; Janek, J. Degradation Mechanisms at the Li₁₀GeP₂S₁₂/LiCoO₂ Cathode Interface in an All-Solid-State Lithium-Ion Battery. *ACS Appl. Mater. Interfaces* **2018**, *10* (26), 22226–22236.
- (19) Ning, Z.; Jolly, D. S.; Li, G.; De Meyere, R.; Pu, S. D.; Chen, Y.; Kasemchainan, J.; Ihli, J.; Gong, C.; Liu, B.; Melvin, D. L. R.; Bonnin, A.; Magdysyuk, O.; Adamson, P.; Hartley, G. O.; Monroe, C. W.; Marrow, T. J.; Bruce, P. G. Visualizing plating-induced cracking in lithium-anode solid-electrolyte cells. *Nat. Mater.* **2021**, *20* (8), 1121–1129.
- (20) Yuan, C.; Lu, W.; Xu, J. Unlocking the Electrochemical–Mechanical Coupling Behaviors of Dendrite Growth and Crack Propagation in All-Solid-State Batteries. *Adv. Energy Mater.* **2021**, *11*, 2101807.
- (21) Cabana, J.; Kwon, B. J.; Hu, L. Mechanisms of Degradation and Strategies for the Stabilization of Cathode–Electrolyte Interfaces in Li-Ion Batteries. *Acc. Chem. Res.* **2018**, *51* (2), 299–308.
- (22) Keller, M.; Varzi, A.; Passerini, S. Hybrid electrolytes for lithium metal batteries. *J. Power Sources* **2018**, *392*, 206–225.
- (23) Merrill, L. C.; Chen, X. C.; Zhang, Y.; Ford, H. O.; Lou, K.; Zhang, Y.; Yang, G.; Wang, Y.; Wang, Y.; Schaefer, J. L.; Dudney, N. J. Polymer–Ceramic Composite Electrolytes for Lithium Batteries: A Comparison between the Single-Ion-Conducting Polymer Matrix and Its Counterpart. *ACS Applied Energy Materials* **2020**, *3* (9), 8871–8881.
- (24) Agapov, A. L.; Sokolov, A. P. Decoupling Ionic Conductivity from Structural Relaxation: A Way to Solid Polymer Electrolytes? *Macromolecules* **2011**, *44* (11), 4410–4414.
- (25) Wang, Y.; Agapov, A. L.; Fan, F.; Hong, K.; Yu, X.; Mays, J.; Sokolov, A. P. Decoupling of Ionic Transport from Segmental Relaxation in Polymer Electrolytes. *Phys. Rev. Lett.* **2012**, *108* (8), 088303.
- (26) Singh, M.; Odusanya, O.; Wilmes, G. M.; Eitouni, H. B.; Gomez, E. D.; Patel, A. J.; Chen, V. L.; Park, M. J.; Fragouli, P.; Iatrou, H.; Hadjichristidis, N.; Cookson, D.; Balsara, N. P. Effect of Molecular Weight on the Mechanical and Electrical Properties of Block Copolymer Electrolytes. *Macromolecules* **2007**, *40* (13), 4578–4585.
- (27) Kim, O.; Kim, K.; Choi, U. H.; Park, M. J. Tuning anhydrous proton conduction in single-ion polymers by crystalline ion channels. *Nat. Commun.* **2018**, *9* (1), 5029.
- (28) Lascaud, S.; Perrier, M.; Vallee, A.; Besner, S.; Prud'homme, J.; Armand, M. Phase Diagrams and Conductivity Behavior of Poly(ethylene oxide)-Molten Salt Rubbery Electrolytes. *Macromolecules* **1994**, *27* (25), 7469–7477.
- (29) Keith, J. R.; Ganesan, V. Ion transport mechanisms in salt-doped polymerized zwitterionic electrolytes. *J. Polym. Sci.* **2020**, *58* (4), 578–588.
- (30) Irfan, M.; Zhang, Y.; Yang, Z.; Su, J.; Zhang, W. Novel conducting solid polymer electrolytes with a zwitterionic structure boosting ionic conductivity and retarding lithium dendrite formation. *Journal of Materials Chemistry A* **2021**, *9*, 22878.
- (31) Lu, F.; Gao, X.; Wu, A.; Sun, N.; Shi, L.; Zheng, L. Lithium-Containing Zwitterionic Poly(Ionic Liquid)s as Polymer Electrolytes for Lithium-Ion Batteries. *J. Phys. Chem. C* **2017**, *121* (33), 17756–17763.
- (32) Lu, F.; Li, G.; Yu, Y.; Gao, X.; Zheng, L.; Chen, Z. Zwitterionic impetus on single lithium-ion conduction in solid polymer electrolyte for all-solid-state lithium-ion batteries. *Chemical Engineering Journal* **2020**, *384*, 123237.
- (33) Taylor, M. E.; Panzer, M. J. Fully-Zwitterionic Polymer-Supported Ionogel Electrolytes Featuring a Hydrophobic Ionic Liquid. *J. Phys. Chem. B* **2018**, *122* (35), 8469–8476.
- (34) D'Angelo, A. J.; Panzer, M. J. Design of Stretchable and Self-Healing Gel Electrolytes via Fully Zwitterionic Polymer Networks in Solvate Ionic Liquids for Li-Based Batteries. *Chem. Mater.* **2019**, *31* (8), 2913–2922.
- (35) Sun, J.; MacFarlane, D. R.; Byrne, N.; Forsyth, M. Zwitterion effect in polyelectrolyte gels based on lithium methacrylate-*N,N*-dimethyl acrylamide copolymer. *Electrochim. Acta* **2006**, *51* (19), 4033–4038.
- (36) Guzmán, G.; Nava, D. P.; Vazquez-Arenas, J.; Cardoso, J. Design of a Zwitterion Polymer Electrolyte Based on Poly[*poly*(ethylene glycol) methacrylate]: The Effect of Sulfobetaine Group on Thermal Properties and Ionic Conduction. *Macromol. Symp.* **2017**, *374* (1), 1600136.

- (37) Makhlooghiyazad, F.; O'Dell, L. A.; Porcarelli, L.; Forsyth, C.; Quazi, N.; Asadi, M.; Hutt, O.; Mecerreyes, D.; Forsyth, M.; Pringle, J. M. Zwitterionic materials with disorder and plasticity and their application as non-volatile solid or liquid electrolytes. *Nat. Mater.* **2021**, DOI: 10.1038/s41563-021-01130-z.
- (38) Mei, W.; Rothenberger, A. J.; Bostwick, J. E.; Rinehart, J. M.; Hickey, R. J.; Colby, R. H. Zwitterions Raise the Dielectric Constant of Soft Materials. *Phys. Rev. Lett.* **2021**, *127* (22), 228001.
- (39) Walden, P. Innere Reibung und deren Zusammenhang mit dem Leitvermögen. *Z. Phys. Chem.* **1906**, *55U* (2), 207–249.
- (40) Floudas, G.; Placke, P.; Stepanek, P.; Brown, W.; Fytas, G.; Ngai, K. L. Dynamics of the "Strong" Polymer of n-Lauryl Methacrylate below and above the Glass Transition. *Macromolecules* **1995**, *28* (20), 6799–6807.
- (41) Floudas, G.; Štěpánek, P. Structure and Dynamics of Poly(n-decyl methacrylate) below and above the Glass Transition. *Macromolecules* **1998**, *31* (20), 6951–6957.
- (42) Köberle, P.; Laschewsky, A.; Tsukruk, V. The structural order of some novel ionic polymers, 1. X-ray scattering studies. *Makromol. Chem.* **1992**, *193* (8), 1815–1827.
- (43) Galin, M.; Marchal, E.; Mathis, A.; Galin, J.-C. Poly(ammonioalkanesulfonate) Blends with Polar Organic Species and Alkali Metal Salts: Structure, Glass Transition and Ionic Conductivity. *Polym. Adv. Technol.* **1997**, *8* (2), 75–86.
- (44) Lee, C.-U.; Li, A.; Ghale, K.; Zhang, D. Crystallization and Melting Behaviors of Cyclic and Linear Polypeptoids with Alkyl Side Chains. *Macromolecules* **2013**, *46* (20), 8213–8223.
- (45) Chintapalli, M.; Timachova, K.; Olson, K. R.; Mecham, S. J.; Devaux, D.; DeSimone, J. M.; Balsara, N. P. Relationship between Conductivity, Ion Diffusion, and Transference Number in Perfluoropolyether Electrolytes. *Macromolecules* **2016**, *49* (9), 3508–3515.
- (46) Schausser, N. S.; Sanoja, G. E.; Bartels, J. M.; Jain, S. K.; Hu, J. G.; Han, S.; Walker, L. M.; Helgeson, M. E.; Seshadri, R.; Segalman, R. A. Decoupling Bulk Mechanics and Mono- and Multivalent Ion Transport in Polymers Based on Metal–Ligand Coordination. *Chem. Mater.* **2018**, *30* (16), 5759–5769.
- (47) Mindemark, J.; Lacey, M. J.; Bowden, T.; Brandell, D. Beyond PEO—Alternative host materials for Li⁺-conducting solid polymer electrolytes. *Prog. Polym. Sci.* **2018**, *81*, 114–143.
- (48) Robeson, L. M. Correlation of separation factor versus permeability for polymeric membranes. *J. Membr. Sci.* **1991**, *62* (2), 165–185.